Fluorescence Properties of DNA Nucleosides and Nucleotides: A Refined Steady-State and Femtosecond Investigation

D. Onidas, D. Markovitsi,* S. Marguet, A. Sharonov, and T. Gustavsson*

Laboratoire Francis Perrin (CNRS URA 2453), DSM/DRECAM/SPAM, CEA Saclay, 91191 Gif-sur-Yvette, France

Received: May 3, 2002; In Final Form: August 1, 2002

The room-temperature fluorescence properties of DNA nucleoside and nucleotide aqueous solutions are studied by steady-state and time-resolved spectroscopy. The steady-state fluorescence spectra, although peaking in the near-UV region, are very broad, extending over the whole visible domain. Quantum yields are found to be mostly higher and the fluorescence decays faster than those reported in the literature. The fluorescence spectra of the 2′-deoxynucleosides are identical to those of the 2′-deoxynucleotides, with the exception of 2′-deoxyadenosine, for which a difference in the spectral width is observed. The steady-state absorption and fluorescence spectra do not show any concentration dependence in the range 5×10^{-6} to 2×10^{-3} M. All fluorescence decays are complex and cannot be described by monoexponential functions. From the zero-time fluorescence anisotropies recorded at 330 nm, it is deduced that after excitation at 267 nm the largest modification in the electronic structure is exhibited by 2′-deoxyguanosine. In the case of purines, the fluorescence decays and quantum yields are the same for 2′-deoxynucleosides and 2′-deoxynucleotides. In contrast, for pyrimidines, the fluorescence quantum yields of nucleotides are higher and the fluorescence decays slower as compared to those of the corresponding nucleosides showing that the phosphate moiety affects the excited-state relaxation.

1. Introduction

DNA fluorescence may provide precious information for the understanding of various aspects of the double helix at the molecular level, such as local motions[1] but also the primary photoinduced processes responsible for lethal or mutagenic effects on the cells.[2−6] One strategy to this end consists of comparing fluorescence that originates from oligonucleotides or polynucleotides to that of their monomeric units and analyzing them with appropriate theoretical models.[7−9] Such a comparison is meaningful only if the monomer properties are described with a good precision and the relaxation processes occurring in the first singlet excited state are sufficiently well understood. These two requisites are still not fulfilled today despite the fact that fluorescence studies of DNA and its components started more than 30 years ago.[10,11]

Early measurement of nucleoside and nucleotide fluorescence spectra gave varying results, notably regarding the quantum yields.[12−14] In the course of time, the values determined in different laboratories converged to about 10^{-4}.[15,16] Even so, the ordering of the various compounds with respect to this property is still not clear. It is worth mentioning, however, that all published fluorescence spectra are restricted in the near-UV and blue region although their red wing seems to extend further into the visible. Such a truncation may affect the quantum yield values. A good characterization of the red wing is particularly important for the study of double-stranded structures, which may fluoresce at longer wavelengths compared to the monomers.[7,9]

Regarding the fluorescence dynamics of DNA components, an evaluation was made on the basis of steady-state measurements: because fluorescence of aqueous solutions was found to be polarized at room temperature,[17−19] the fluorescence lifetimes should be shorter than the characteristic time for rotational diffusion. Thus, lifetimes on the order of 1 ps or less were expected,[15] but direct measurements of fluorescence decays remained a real challenge for a long time because they necessitated subpicosecond resolution. With the development of femtosecond lasers, a few attempts to characterize fluorescence decays using streak cameras were made, but these yielded only upper limits of the lifetimes because the instrumental response functions were of several picoseconds.[20,21]

The first femtosecond fluorescence studies of DNA components appeared only a few months ago.[22−24] They were performed using the upconversion technique based on the mixing of fluorescence with an ultrashort laser pulse in a nonlinear crystal. Peon and Zewail reported that the excited-state lifetimes of DNA/RNA nucleosides and nucleotides all fall in the subpicosecond time scale and that the lifetimes of the nucleotides are longer than those of the corresponding nucleosides up to 20%.[22] In parallel, we investigated the adenine and thymine homologous series comparing the base properties to those of the corresponding nucleoside and nucleotide.[23,24] Our results corroborated those by Peon and Zewail about the fact that thymidine fluorescence decays faster than that of thymidine-5′-monophosphate whereas no such distinction can be made in the adenine series. But in contrast to ref 22, our work revealed that the fluorescence decays are complex and cannot be described by single exponentials. The most important difference between the two studies concerns 2′-deoxyadenosine for which we found that 76% of the fluorescence disappears within less than 100 fs, while a lifetime of 530 ± 120 fs is given in ref 22. Interestingly, transient absorption experiments yielded a lifetime of only 290 fs for the first singlet excited state of 2′-deoxyadenosine.[25] Given the above-mentioned discrepancies in the results obtained by the upconversion technique, the question arises whether the fluorescence decays of 2′-deoxycytidine, 2′-

10.1021/jp026063g CCC: $22.00
Published on Web 10/04/2002

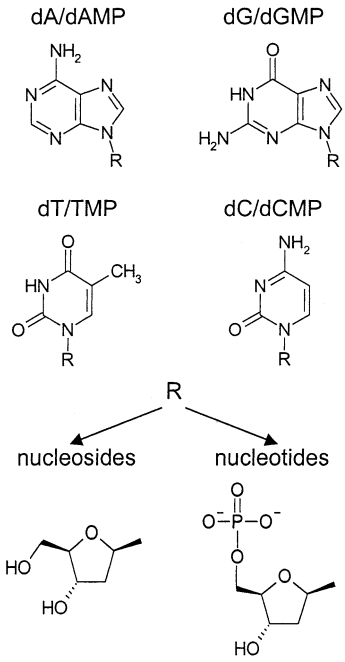

Figure 1. The DNA nucleosides and nucleotides.

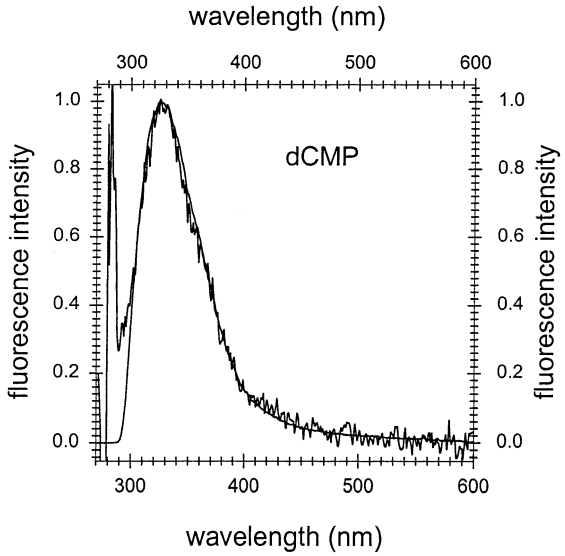

Figure 2. Normalized fluorescence spectra of concentrated (2×10^{-3} M) and dilute (10^{-5} M; noisy line) dCMP aqueous solutions. $\lambda_{ex} =$ 255 nm.

deoxyguanosine, and their nucleotides also contain ultrafast components.

Moreover, the combination of steady-state and time-resolved fluorescence data can bring some insight in the excited-state relaxation. In an ideal case, in which emission originates from the directly excited state, the radiative lifetime of a chromophore can be easily calculated as the ratio between the fluorescence lifetime and the quantum yield. In contrast, if the fluorescent state is not directly populated, such a relationship is not fulfilled. Thus, it would be interesting to examine how nucleosides and nucleotides compare in this respect.

For these reasons, we have decided to pursue our femtosecond investigation of DNA nucleosides and nucleotides by means of the upconversion technique, providing both fluorescence decays and fluorescence anisotropy decays. In parallel, we have undertaken a refined study of the same compounds using steady-state absorption and fluorescence spectroscopy. The developments made in commercial spectrofluorometers since the first fluorescence measurements of DNA components give the possibility to improve the quality of the emission spectra. Our aim was to provide steady-state and time-resolved data with improved precision.

The present paper is focused on DNA derivatives (Figure 1): 2′-deoxyadenosine (dA), 2′-deoxyadenosine-5′-monophosphate (dAMP), thymidine (dT), thymidine-5′-monophosphate (TMP), 2′-deoxyguanosine (dG), 2′-deoxyguanosine-5′-monophosphate (dGMP), 2′-deoxycytidine (dC), and 2′-deoxycytidine-5′-monophosphate (dCMP). We present absorption and fluorescence spectra obtained for aqueous solutions of commercially available compounds. Because femtosecond experiments are carried out with relatively concentrated solutions, we also examine the concentration effect over a range from 5×10^{-6} to 2×10^{-3} M.

2. Experimental Details

Materials. DNA nucleosides and nucleotides (disodium salts), as well as thymine, were purchased from Sigma Aldrich and used without further purification. For the determination of the molar extinction coefficients, dCMP and dGMP were dried at 50 °C for 5 h under vacuum (1 mbar). The nucleosides dA, dC, and dG from ICN Biochemicals GmbH were also tested and gave the same absorption and fluorescence spectra as those from Sigma Aldrich. The compounds were dissolved in ultrapure water produced by a MILLIPORE (Milli-Q Synthesis) purification system. Particular caution (pyrolysis, rinsing with ultrapure water) was necessary not to contaminate the glass vessels with fluorescent impurities. Before using water for solution preparation, we systematically left flowing about 4 L from the purification system. Under these conditions, the "spectra" recorded for ultrapure water consisted of the main Raman line followed by a weak continuum.

Dihydrate quinine sulfate and 2,5-diphenyloxazole (PPO) were obtained from Prolabo and Sigma Aldrich, respectively.

Steady-State Measurements. Absorption spectra were recorded with a Perkin Lamda 900 spectrophotometer using 1 mm, 2 mm, 1 cm, and 5 cm quartz cells (QZS).

Fluorescence spectra were recorded with a SPEX Fluorolog-2 spectrofluorometer. The light source was a 450 W arc xenon lamp. Emission spectra were recorded with a band-pass of 4.71 nm at excitation side and 2.25 nm at the emission side. The calibration of the emission monochromator was verified using a Hg low-pressure standard lamp, whereas that of the excitation monochromator was confirmed by observing the scattered excitation light from water. The emission correction factor was performed by means of deuterium and tungsten lamps of standard irradiance and checked via the standard fluorescence spectrum of quinine sulfate.[26]

For fluorescence measurements, 1 cm × 1 cm and 0.2 cm × 1 cm quartz cells (QZS) were used for dilute and concentrated solutions, respectively. For dilute solutions ($<5 \times 10^{-5}$ M), the water signal was not negligible compared to the fluorescence intensity. Therefore, its contribution was subtracted from the fluorescence spectra. In this way, the weak continuum was removed but the main Raman line could not be completely eliminated (Figure 2). To obtain the emission spectrum of a given solution over the whole near-UV and visible area, each spectrum was recorded three times: (i) without any filter at the emission side and using (ii) a Schott WG320 or (iii) a Schott GG385 filter. In all cases, a Schott UG5 filter was used on the excitation side. The three spectra were normalized at appropriate wavelengths and then joined. Such a procedure allowed us to eliminate the second order of the scattered excitation light from

water, Raman scattering, and also the second order of the main fluorescence peak. Such a procedure allowed us to record reliable fluorescence emission spectra over a large spectral domain. In contrast, we did not succeed so far to record fluorescence excitation spectra with the same precision. The reason is that excitation spectra have to be recorded for solutions with optical densities lower than 0.05 in the spectral domain 230−300 nm. Under these conditions, it is difficult to eliminate the optical artifacts mentioned above. Thus, we have the feeling that our excitation spectra are not any better than those reported earlier. Therefore, we are not able to make any refined comparison between absorption and excitation spectra.

Fluorescence quantum yields (ϕ_x) were determined using quinine sulfate dihydrate in 0.1 M $HClO_4$ ($\phi_s = 0.59$).[26] As a control, the fluorescence quantum yield of PPO in cyclohexane was determined and found to be 0.90 ± 0.02, in perfect agreement with the most recent value reported in the literature (0.89).[27]

Time-Resolved Measurements. The fluorescence upconversion setup is described in detail elsewhere.[23,24] Briefly, the third harmonic of a mode-locked Ti−sapphire laser (267 nm) was used for excitation. The spectral resolution at the detection wavelength (223−244 nm) was set to 8 nm. Parallel (I_{par}) and perpendicular (I_{perp}) excitation/detection configurations were realized by controlling the polarization of the exciting beam with a half-wave plate. Fluorescence decays were typically recorded at 310, 330, 350, and 370 nm. Temporal scans were made in an 8 ps time window with 33.3 fs steps in both parallel and perpendicular configurations.

The apparatus function was determined by measuring either the rise time in the blue wing (320−340 nm) of the fluorescence from a dimethylquaterphenyl (Lambda Physics) solution in cyclohexane or the width (fwhm) of the dominant Raman line in water at 296 nm. In both cases, the apparatus function was found to be around 450 fs (fwhm). We judge that the time resolution of our set up is 100 fs after deconvolution.

Solutions (5×10^{-4} to 2×10^{-3} M) were kept flowing in a 0.4 mm quartz cell, which itself was kept in continuous motion perpendicular to the excitation beam. The power density was estimated to be 0.2 ± 0.1 GW/cm^2 for a 50 mW output from the tripler unit. Successive recordings with the same solution gave reproducible signals, showing that photodegradation does not affect our measurements.

All measurements were performed at room temperature (20 ± 1 °C) under aerated conditions.

3. Results

Steady-State Measurements. The absorption spectra of 2′-deoxynucleosides are shown in Figure 3. It is worth noticing that they nearly cross at 271 nm where the molar extinction coefficients are 9300 ± 250 cm^{-1}. The absorption maxima (λ_{max}) and the corresponding extinction coefficients (ϵ_{max}) are given in Table 1. The normalized spectra of the 2′-deoxynucleotides are identical to those of the nucleosides, but their extinction coefficients were found to be somewhat weaker. The absorption spectra of all eight compounds do not show any concentration dependence in the range 5×10^{-6} to 2×10^{-3} M.

We recorded fluorescence spectra by exciting at wavelengths ranging from 240 to 280 nm with the exception of dA and dAMP for which excitation wavelengths ranged from 240 to 267 nm. We found that the spectrum profile of each compound was practically the same for all excitation wavelengths; the only noticeable difference was a weak broadening (ca. 5% of fwhm on a nanometer scale) on the red side of the fluorescence band when exciting at the 240−245 nm domain.

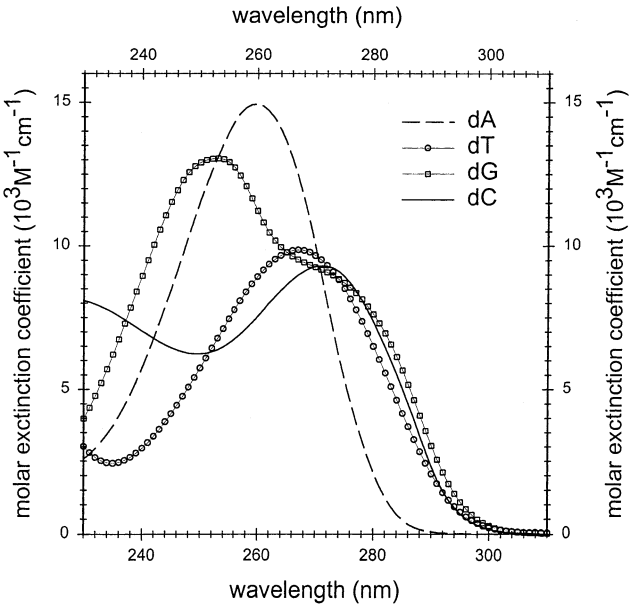

Figure 3. Electronic absorption spectra recorded for 2′-deoxynucleosides in water.

TABLE 1: Characteristics of the Absorption Spectra of DNA Nucleoside and Nucleotide Aqueous Solutions

compd	λ_{max}[a,d] (nm)	ϵ_{max}[b,d] (10^3 M^{-1} cm^{-1})
dA	259.7 (259.5)	14.93 (14.9)[c]
dAMP	259.7 (260)	14.69 (15.0)[c]
dT	267.0 (267)	9.86 (9.7)
TMP	267.3 (268)	9.50 (9.5)
dC	270.7 (272)	9.30 (9.1)
dCMP	271.7 (272)	8.80 (9.3)[c]
dG	252.7 (252.5)	13.85 (13.7)[c]
dGMP	253.1 (252.5)	13.53 (13.5)[c]

[a] Error = ±0.2 nm. [b] Error = ±150 M^{-1} cm^{-1}. [c] Determined for the ribonucleosides. [d] Values in parentheses were reported in ref 28.

Regarding the concentration dependence, we did not detect any spectral variation, apart from reabsorption on the blue side, when going from 5×10^{-6} to 2×10^{-3} M; an example is shown in Figure 2 for dCMP. The spectrum profile on the blue side was obtained by exciting dilute solutions at 240 nm (circles in Figure 4) because for this excitation wavelength the intense Raman line does not distort the spectrum.

A main feature of the fluorescence spectra shown in Figure 4 is that, although they peak between 305 and 335 nm, they all present a long tail that extends over the whole visible area. The normalized fluorescence spectra of dC, dG, and dT are identical to those of dCMP, dGMP, and TMP, respectively. In contrast, the red wing tail observed for dA is more intense than the dAMP one. For example, at 400 nm, the intensity of the dA fluorescence is 50% higher compared to that of the dAMP.

The fluorescence quantum yield is given by

$$\phi_x = \frac{A_x}{A_s}\frac{(1-10^{-OD_s})}{(1-10^{-OD_x})}\frac{n_x^2}{n_s^2}\phi_s \qquad (1)$$

where A is the area of the spectrum, OD the optical density of the solution at the exciting wavelength, and n the refraction index of the solution. The subscripts x and s denote, respectively, the studied compound and the fluorescence standard. We found

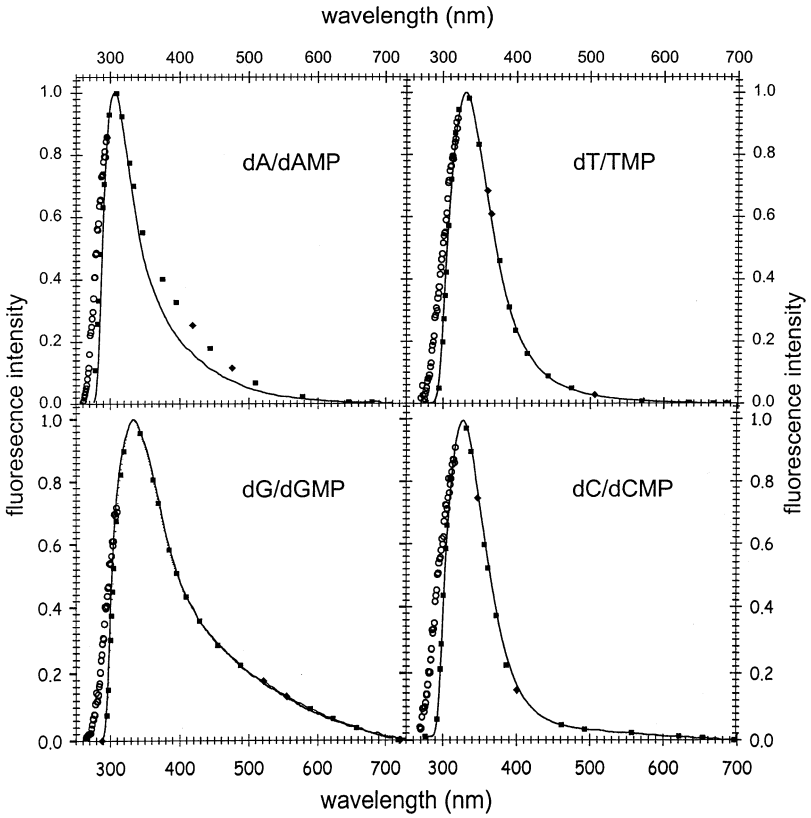

Figure 4. Fluorescence spectra of 2′-deoxynucleotides (solid lines) and 2′-deoxynucleosides (dotted lines) recorded for 2×10^{-3} M aqueous solutions. $\lambda_{ex} = 255$ nm. The circles correspond to the spectra of dilute solutions (2×10^{-6} to 10^{-5} M) excited at 240 nm to avoid distortion due to the Raman line.

that a better precision in the determination of the ϕ values could be achieved by decomposing the area of the spectrum as $A = A_n I_{max}$, where A_n is the area of the spectrum of which the maximum intensity is normalized to unity and I_{max} is the maximum intensity of the fluorescence spectrum. The spectral areas A_n were obtained according to the procedure described in section 2, that is, constructed from three separate recordings with different filters and corrected for the reabsorption in the blue wing. They correspond to the spectra shown in Figure 4 and include the blue-side part obtained upon excitation at 240 nm. When the emission spectra are recorded every 1 nm, A_n was found to be equal to 99, 83, 81, 77, and 130, (error of ± 4) for dA, dAMP, dT/TMP, dC/dCMP, and dG/dGMP, respectively. A mean value of I_{max} was determined from a series of spectra recorded for different dilute solutions ($< 5 \times 10^{-5}$ M). We determined the fluorescence quantum yields by exciting at 255 nm. For this wavelength, the spectra are strictly identical to those obtained upon excitation at 267 nm, allowing a straightforward comparison with the fluorescence decays. Moreover, it permits us to determine I_{max} with a good precision, which is not possible when exciting at 267 nm because the Raman line is too close to the fluorescence maximum.

At this point, we can make two remarks. First, optical artifacts, which we tried to eliminate as described in section 2, tend to increase A_n and thus ϕ. Second, the quantum yield values determined for solutions with optical densities at the excitation wavelength ranging from 0.04 to 0.6 were the same within the error bars; for higher OD, ϕ appeared to decrease. The quantum yield values obtained for the DNA nucleotides and nucleosides are presented in Table 2; they range between 0.7×10^{-4} (dAMP) and 1.5×10^{-4} (TMP).

Time-Resolved Measurements. Figure 5 shows the fluorescence decays recorded for 2×10^{-3} M aqueous solution of

TABLE 2: Fluorescence Maxima (λ_{fl}) and Fluorescence Quantum Yields (ϕ) of DNA Nucleoside and Nucleotide Aqueous Solutions Determined upon Excitation at 255 nm

compd	λ_{fl} (nm)[a,b]	$\phi \times 10^4$ [a]
dA	307 (312[16], 310[15])	0.86 ± 0.15 (0.6^{16}, 0.5^{15})
dAMP	306 (312)[16]	0.68 ± 0.10 (0.5)[16]
dT	330 (330[16], 327[15])	1.32 ± 0.07 (0.9^{16}, 1.0^{15})
TMP	330 (330[16], 327[15])	1.54 ± 0.11 (1.2^{16}, 1.1^{15})
dC	328 (330[16], 324[15])	0.89 ± 0.10 (0.7^{16}, 0.7^{15})
dCMP	328 (330[16], 324[15], 320[18])	1.15 ± 0.06 (1.2^{16}, 0.84^{15},1.0^{18})
dG	334 (340[16], 346[21])	0.97 ± 0.08 (1^{16})
dGMP	334 (340[16], 346[21])	1.09 ± 0.10 (0.8^{16})

[a] Values reported in the literature for dT, TMP, and the RNA analogues of the other compounds are given in parentheses. [b] Error = ± 1 nm.

dG at 330 nm with parallel and perpendicular excitation/detection configurations. The same type of traces were obtained for the other compounds. These recordings allowed us to determine not only the time dependence of the total fluorescence, $F(t)$, but also that of the fluorescence anisotropy, $r(t)$. To this end, we performed a merged nonlinear fitting/deconvolution process directly on the parallel (I_{par}) and perpendicular (I_{perp}) signals, using the model functions

$$i_{par}(t) = (1 + 2r(t))f(t) \quad (2)$$

$$i_{perp}(t) = (1 - r(t))f(t) \quad (3)$$

convoluted with a Gaussian apparatus function; $r(t)$ and $f(t)$ can be exponential decay functions of arbitrary order.

Total fluorescence, $F(t)$, kinetics were also constructed from the parallel and perpendicular signals according to the equation

$$F(t) = I_{par}(t) + 2I_{perp}(t) \quad (4)$$

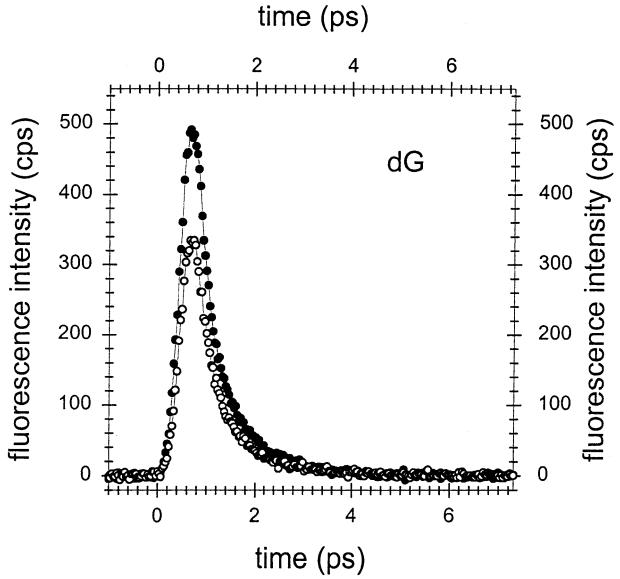

Figure 5. Fluorescence decays recorded for 2×10^{-3} M aqueous solutions of dG at 330 nm after excitation at 267 nm with parallel (upper curve) and perpendicular (lower curve) excitation/detection configurations. Model fitted curves are given as solid lines.

The total fluorescence decay signals obtained for the four 2′-deoxynucleosides at 330 are shown in Figure 6. The same kind of signal was found for the nucleotides. An important remark to make is that the fluorescence decays faster for dC and dT as compared to dCMP and TMP, respectively, while no clear distinction can be made either between the decays of dA and dAMP or those of dG and dGMP.

None of the observed fluorescence decays could be described in a satisfactory way by a single exponential. In contrast,

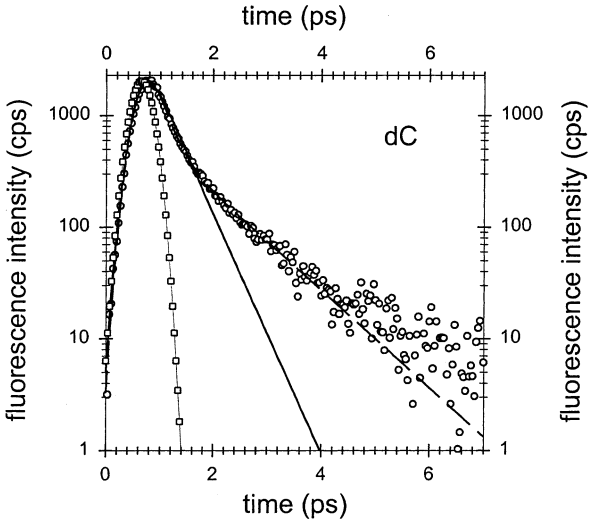

Figure 7. Total fluorescence decay of a 2×10^{-3} M aqueous solution of dC at 330 nm (open circles) fitted with a monoexponential (solid line) and biexponential function (dashed line). The instrumental response function is represented by squares; $\lambda_{ex} = 267$ nm.

biexponential functions reproduce the data more adequately. The improvement in the fit quality achieved by a biexponential function compared to a monoexponential one is quantified by the ratio rms_2/rms_1 of the corresponding root-mean-square errors. These ratios can be as large as ca. 40%. To illustrate the clear biexponentiality of $F(t)$, the total fluorescence decay of dC is shown on a semilogarithmic scale in Figure 7. As can be seen, a monoexponential function strongly deviates from experimental data.

In the subsequent fitting procedure using eqs 2 and 3, fully free-floating fits with adjustable apparatus function width and

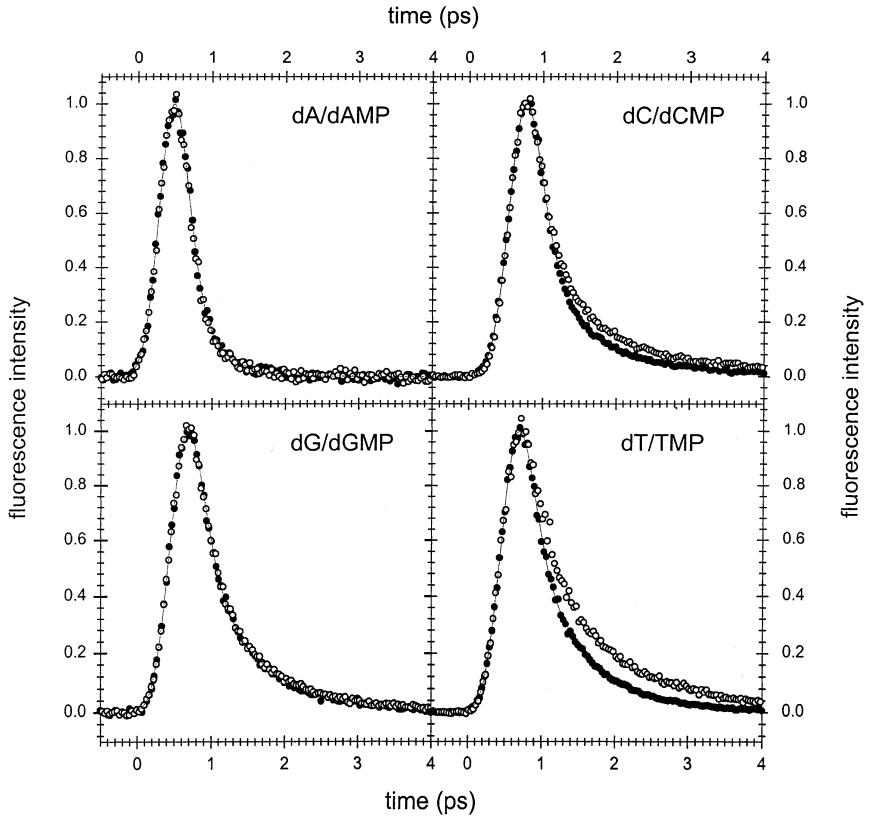

Figure 6. Normalized total fluorescence decays obtained for 2×10^{-3} M aqueous solutions of 2′-deoxynucleosides (solid circles) and 2′-deoxynucleotides (open circles) at 330 nm. $\lambda_{ex} = 267$ nm.

TABLE 3: Characteristic Times (ps) of the Fluorescence Decays of DNA Components at 330 nm Resulting from the Fits with Monoexponential ($\exp(-t/\tau_0)$) and Biexponential Functions ($\alpha \exp(-t/\tau_1) + (1 - \alpha) \exp(-t/\tau_2)$)[a]

compd	τ_0	rms_2/rms_1[b]	τ_1	τ_2	a	p[c]	$\langle\tau\rangle$[e]
dA	0.17 ± 0.01	0.95	0.10[d]	0.42 ± 0.10	0.91 ± 0.01	0.28 ± 0.02	0.13 ± 0.01
dAMP	0.16 ± 0.01	0.92	0.10[d]	0.52 ± 0.10	0.94 ± 0.02	0.25 ± 0.01	0.13 ± 0.01
dT	0.47 ± 0.01	0.61	0.15 ± 0.02	0.72 ± 0.03	0.70 ± 0.02	0.68 ± 0.02	0.32 ± 0.01
TMP	0.68 ± 0.02	0.62	0.21 ± 0.03	1.07 ± 0.06	0.67 ± 0.02	0.72 ± 0.02	0.50 ± 0.02
dC	0.40 ± 0.01	0.58	0.18 ± 0.02	0.92 ± 0.06	0.83 ± 0.02	0.51 ± 0.02	0.30 ± 0.01
dCMP	0.53 ± 0.02	0.66	0.27 ± 0.02	1.38 ± 0.11	0.84 ± 0.02	0.50 ± 0.02	0.45 ± 0.02
dG	0.46 ± 0.01	0.69	0.16 ± 0.02	0.78 ± 0.05	0.73 ± 0.02	0.63 ± 0.02	0.33 ± 0.01
dGMP	0.47 ± 0.01	0.65	0.20 ± 0.02	0.89 ± 0.06	0.79 ± 0.02	0.54 ± 0.02	0.34 ± 0.01

[a] The errors are those resulting from the global fits with an instrumental function fixed at 450 fs. [b] Root-mean-square error obtained for fits with monoexponential (rms_1) and biexponential functions (rms_2). [c] $p = (1 - \alpha)\tau_2/(\alpha\tau_1 + (1 - \alpha)\tau_2)$ corresponds to the relative contribution of the τ_2 component to the time-integrated total fluorescence. [d] Limited by the time-resolution of the system, 0.10 ps after deconvolution. [e] $\langle\tau\rangle = \alpha\tau_1 + (1 - \alpha)\tau_2$.

mono- or biexponential $f(t)$ model functions were performed for individual data sets, all recorded at 330 nm, to judge the consistency of the different rms_2. Regarding the apparatus function, the results were in accordance with the 450 fs width (fwhm), as described in the experimental part. For the anisotropy decays, initially we tested monoexponential functions, $r(t)$; the resulting characteristic times were found to be several tens of picoseconds, which is not significant given the probed time scale (<10 ps). For this reason, we set in the following the characteristic time to 50 ps.

For none of the compounds was any clear wavelength dependence of the decay kinetics observed. So, we focused on the 330 nm runs, and we performed global fits by merging all data obtained for each compound at this wavelength and fixing the apparatus function width to 450 fs. The time constants obtained from monoexponential (τ_0), as well as biexponential fits (τ_1 and τ_2), are given in Table 3; we also present an average value of the decay time calculated as $\langle\tau\rangle = \alpha\tau_1 + (1 - \alpha)\tau_2$. We remark that $\langle\tau\rangle$ is shorter than τ_0. In this table, slightly different values are reported for dA, dAMP, dT, and TMP, compared to those given in refs 23 and 24. The reason is that new experiments with improved signal-to-noise ratio and time-resolution have been performed. However, the variations are small, and the values are the same within the error limits.

For all compounds, biexponential fits yielded one very fast component (τ_1) and a longer one (τ_2). In the case of dA and dAMP, the τ_1 value was smaller than the time resolution of our detection system (100 fs), so we do not judge it significant, and we fixed it to 100 fs. For the other 2′-deoxynucleosides and 2′-deoxynucleotides, this short component was found to be between 0.15 ps for dT and 0.27 ps for dCMP. The slow component ranged from 0.4 ps for dA and dAMP up to 1.4 ps for dCMP. The relative contribution p of the τ_2 component to the total fluorescence corresponds to the major part of the fluorescence for dT and TMP (ca. 70%), while it is only ca. 25% for dA and dAMP. In the latter case, the relative error in the determination of p is high because of the weak amplitude of the slow component.

The zero-time anisotropy of the 2′-deoxynucleosides was found to be the same as that of the corresponding 2′-deoxynucleotides within the precision of our measurements. Those values are shown in Table 4. TMP and dCMP exhibit $r(0)$ values around 0.35; these values, although quite high, are significantly different from the upper limit of 0.4 expected for parallel absorption and emission transition moments. Much lower values are found for dAMP (0.25) and dGMP (0.15).

TABLE 4: Zero-time Fluorescence Anisotropies, $r(0)$, and Steady-State Anisotropies, $\langle r\rangle$, Deduced[a] from Polarization Ratios (P)[29] Observed for 2′-Deoxynucleotides for Excitation at 267 nm and Emission at 330 nm

	dAMP	TMP	dCMP	dGMP
$r(0)$	0.24 ± 0.01	0.36 ± 0.01	0.34 ± 0.01	0.15 ± 0.04
θ[b]	31°	15°	18°	40°
$\langle r\rangle$	0.28	0.43	0.44	0.13

[a] According to the equation $\langle r\rangle = (P - 1)/(P + 2)$. [b] θ denotes the angle between absorption and emission transition moments deduced from $r(0)$ (eq 5).

4. Discussion

In this section, we begin by comparing the results obtained in our study with those reported in the literature. Then, in the light of our steady-state and time-resolved data, we discuss the relaxation of DNA nucleosides and nucleotides in their lowest excited state, as well as the possible deactivation pathways of the emissive state. We also examine the effect of the phosphate group in these processes.

In Table 1, we compare the characteristic features of the absorption spectra determined in the present study to those reported by Voet et al.[28] It is worth noticing that, although the latter publication is widely cited as far as absorption spectra of DNA/RNA components are concerned, it does not contain original data for the molar extinction coefficients of the lowest absorption band, but it quotes values from older, partially unpublished work. However, the wavelengths and molar extinction coefficients corresponding to the maxima of the absorption bands found by us for the 2′-deoxynucleosides and 2′-deoxynucleotides are quite similar to those reported in ref 28 for thymidine and the RNA analogues of 2′-deoxyadenosine, 2′-deoxycytidine, and 2′-deoxyguanosine. The largest difference was observed for dCPM (5.4%); the latter compound is particularly hygroscopic and appeared to be pasty even after drying under vacuum.

In Table 2, we compare the maxima of the steady-state fluorescence spectra and the fluorescence quantum yields of 2′-deoxynucleosides and 2′-deoxynucleotides given in the present study with those reported in the literature. A general remark is that our findings are not radically different from the previous values even though the precise experimental conditions and related errors are not always specified in earlier works. Regarding the fluorescence quantum yields, we observe that our values are mostly larger than the literature values.

In Table 5, we compare the τ_0 values resulting from monoexponential fits of our fluorescence upconversion data with those obtained recently in another laboratory using the same technique.[22] We also compare our τ_0 values with reported S_1 lifetimes as determined by transient absorption measurements.[25] It should be observed that only monoexponential lifetimes are given in refs 22 and 25. A common feature in each one of the three studies is that the singlet excited state of 2′-deoxyadenosine

TABLE 5: Lifetimes (ps) Resulting from Fits of Fluorescence Decays (τ_0, Present Study; τ' from Ref 22) and Transient Absorption Decays (τ'' from Ref 25) of Nucleoside and Nucleotide Aqueous Solutions with Monoexponential Functions

compd	τ_0	τ'^a	τ''^a
dA	0.17	0.53	0.29
dAMP	0.16	0.52	
dT	0.47	0.70	0.54
TMP	0.68	0.98	
dC	0.40	0.76	0.72
dCMP	0.53	0.95	
dG	0.46	0.69	0.46
dGMP	0.47	0.86	

[a] Values determined for dT, TMP, and the RNA analogues of the other compounds.

has the shortest lifetime compared to the other nucleosides. All of our τ_0 values are shorter than the lifetimes reported in ref 22, the ratio ranges from 1.4 to up to 3 for dA and dAMP. Our τ_0 values are somewhat closer to those found by transient absorption. Interestingly, the excited-state lifetimes obtained from transient absorption experiments are intermediate between the values of the short and long components (τ_1 and τ_2 in Table 3) resulting from the fit of our data with biexponential functions, while the literature upconversion values are closer to our τ_2 values.

Finally, in Table 4, we compare the nucleotide zero-time anisotropies, $r(0)$, with the findings from low-temperature steady-state polarization measurements.[29] To this end, we have converted the polarization ratios, $P = I_{par}/I_{perp}$, given in that investigation for excitation at 267 nm and emission at 330 nm (1.8, 2.5, 2.6, and 1.3 for dAMP, TMP, dCMP, and dGMP, respectively) to the corresponding anisotropy values, $\langle r \rangle$. It may be remarked that both the steady-state and the time-resolved anisotropies are alike. Notably, they decrease in the order TMP $\approx$ dCMP > dAMP > dGMP.

The small $r(0)$ values, in agreement with the low-temperature steady-state $\langle r \rangle$ values, found for the purines (dA/dAMP and dG/dGMP) prove that an important change in electronic structure takes place after photon absorption, at times below our temporal resolution. This does not seem to be the case for the pyrimidines (dC/dCMP and dT/TMP). A quantitative measure of this rearrangement can be obtained by calculating the average angle θ between the absorption and emission transition dipoles via the formula

$$r = (3 \cos^2 \theta - 1)/5 \qquad (5)$$

The resulting angles are presented in Table 4. Before commenting on these values, it is useful to recall that each absorption spectrum shown in Figure 3 is constituted by several overlapping bands corresponding to different electronic transitions. A decomposition of the 2′-deoxynucleoside absorption spectra is described in detail in ref 30. According to this spectral analysis, excitation at 267 nm populates directly the S_1 state of thymidine, 2′-deoxycytidine, and 2′-deoxyguanosine, while in 2′-deoxyadenosine, it generates a mixture of S_1 and the S_2 (at a ratio of ca. $^1/_3$:$^2/_3$).

The small θ values calculated from eq 5 for the pyrimidines are in line with excitation of and emission from the same electronic state undergoing only vibrational relaxation. The higher θ values found for the purines are more difficult to explain. For 2′-deoxyadenosine, the θ value of 31° is only an average value due to S_1 and the S_2 mixture created upon excitation. Assuming that dA/dAMP fluorescence originates only from S_1 after $S_2 \rightarrow S_1$ internal conversion, we deduce an angle of 37° between the $S_0 \rightarrow S_2$ and $S_1 \rightarrow S_0$, transition dipoles. This angle of 37° is calculated from eq 5 using the above-mentioned ratio of $^1/_3$:$^2/_3$ and assuming that the $r(0)$ value corresponding to fluorescence from the directly excited S_1 state is 0.35 (vibrational relaxation as in the case of the pyrimidines). A comparison with theoretical data is, however, not straightforward because of the great discrepancy among the theoretical values ranging between 36° and 110° (see Table 2 in ref 30). Finally, the spectral analysis performed in ref 30 for 2′-deoxyguanosine does not allow an interpretation analogue to the 2′-deoxyadenosine case. The calculated angle, $\theta = 40°$, shows clearly that an important electronic relaxation takes place after excitation, but we have no hint at its nature.

TABLE 6: Fluorescence Quantum Yields (ϕ), Mean Fluorescence Lifetimes ($\langle \tau \rangle$, ps), Radiative Lifetimes ($\tau_{rad} = \langle \tau \rangle / \phi$, ns), and Stokes Shifts (cm^{-1}) of DNA Nucleoside and Nucleotide Aqueous Solutions

	compd	$\phi \times 10^4$	$\langle \tau \rangle$	τ_{rad}	Stokes shift[a]
purines	dA	0.86 ± 0.15	0.13 ± 0.01	1.5 ± 0.4	4000[b]
	dAMP	0.68 ± 0.10	0.13 ± 0.01	1.9 ± 0.4	
	dG	0.97 ± 0.08	0.33 ± 0.01	3.4 ± 0.4	6800 ± 200[c]
	dGMP	1.09 ± 0.10	0.34 ± 0.01	3.1 ± 0.4	
pyrimidines	dC	0.89 ± 0.10	0.30 ± 0.01	3.4 ± 0.4	6500 ± 100[c]
	dCMP	1.15 ± 0.06	0.45 ± 0.02	3.9 ± 0.3	
	dT	1.32 ± 0.07	0.32 ± 0.01	2.4 ± 0.3	7200 ± 100
	TMP	1.54 ± 0.11	0.50 ± 0.02	3.2 ± 0.4	

[a] Energy difference between the absorption maximum corresponding to $S_0 \rightarrow S_1$ and the fluorescence maximum. [b] $S_0 \rightarrow S_1$ energy taken from ref 33. [c] From ref 30.

The Stokes shift found for dC/dCMP, dG/dGMP, and dT/TMP (Table 6) is very large ($6500-7100\ cm^{-1}$) showing that, in all cases, an enormous stabilization in energy takes place extremely rapidly. The Stokes shift of dA/dAMP is much smaller ($4000\ cm^{-1}$), and it is tempting to relate this with their weaker fluorescence quantum yields and faster fluorescence decays. A final remark concerning the nature of the emitting state is that the radiative lifetimes, estimated as $\tau_{rad} = \langle \tau \rangle / \phi$, range from 1 to 4 ns (Table 6), proving that, for all of the examined compounds, the fluorescence corresponds to an allowed transition.

All of the steady-state fluorescence spectra presented in Figure 4, are very broad, displaying spectral widths amounting to $6000-7000\ cm^{-1}$ (fwhm) with long wavelength tails extending over the whole visible region. Such a behavior may be understood in terms of the lifetime of the fluorescent state being much too short for a vibrational thermalization to occur. Thus, emission emanates from a nonequilibrated excited-state population distributed over many hot vibrational levels. Indeed, this view is in accordance with the fact that the fluorescence bandwidth increases with the excitation energy as mentioned in section 2. Regarding the difference in the fluorescence spectra of dA and dAMP, it arises probably from the fact that the fluorescence band is not homogeneous, as suggested by the steady-state fluorescence anisotropy, which is not constant along the fluorescence spectrum of dAMP.[29]

At this point, it is interesting to examine, in a more general way, the effect of the phosphate group on the fluorescence properties of the DNA components. We have seen that both the fluorescence steady-state spectra (with the exception of the spectral bandwidth just discussed for dA/dAMP) and the zero-time anisotropy values determined for the 2′-deoxynucleosides are the same as those found for the corresponding 2′-deoxynucleotides. The estimated radiative lifetimes are also quite

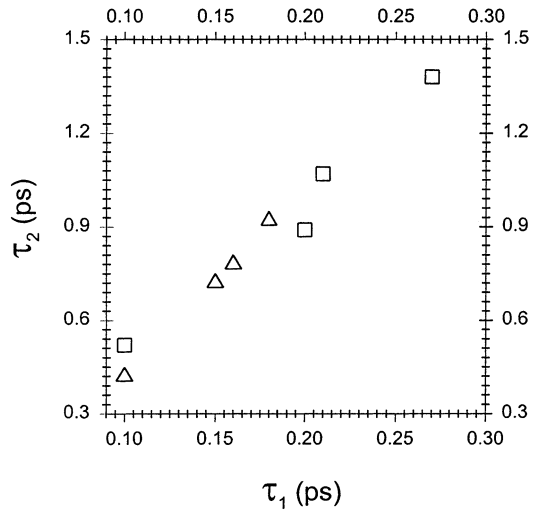

Figure 8. Correlation between the fast (τ_1) and slow (τ_2) components determined for the fit of fluorescence decays at 330 nm of 2′-deoxynucleosides (triangles) and 2′-deoxynucleotides (squares) by biexponential functions.

similar (Table 6). This means that the phosphate moiety does not affect the nature of the emitting state.

Regarding the fluorescence quantum yields and the fluorescence kinetics, we can make a clear distinction between purines and pyrimidines (Table 6). For the former compounds, addition of the phosphate moiety does not induce any noticeable change in the fluorescence decays (Figure 6); moreover, the quantum yields of dG and dGMP are similar, within the experimental precision, as are those of dA and dAMP. In contrast, in the case of pyrimidines, it is clear that fluorescence decays faster for the 2′-deoxynucleosides than for the corresponding 2′-deoxynucleotides; the same difference is observed for the quantum yields, which are found to be higher for dCMP and TMP as compared to dC and dT, respectively. Thus, the phosphate group does play a role in the deactivation of the emitting state in the case of pyrimidines, but it seems to have no influence in the case of purines. We could speculate that such an effect is due to the smaller size of pyrimidines allowing the side group to interact, possibly through hydrogen bonding, with the chromophores.

As developed in section 3, the quality of the fit of all the fluorescence decays significantly improves when going from monoexponential to biexponential functions. Nevertheless, we remark in Figure 8 that there is a clear correlation between the fast and slow component: as τ_1 becomes longer, τ_2 becomes longer. Such a correlation suggests that the underlying physical process does not necessarily correspond to two distinct relaxation pathways. Thus, the apparent lifetimes resulting from fits with monoexponential functions should depend on the time resolution.

The observed nonexponential decays may be of intra- or intermolecular origin. It could involve an inhomogeneous relaxation of the emitting state; for example, hot vibrational levels could relax more rapidly, but this is not supported by the absence of wavelength dependence in the observed kinetics. However, more time-resolved data in the visible region are needed to judge whether such a hypothesis is acceptable. The nonexponentiality of the fluorescence decays could also be due to some complex deactivation path involving several electronic excited states or proton or hydrogen exchange between the chromophore and surrounding water molecules or both.[31,32]

In conclusion, the new experimental results reported in the present study have contributed to clarifying a few points concerning the fluorescence of DNA nucleosides and nucleotides. Our most important findings are that the phosphate moiety plays a role in the deactivation of the lowest excited singlet state of the pyrimidines and that the mechanisms behind the nonradiative relaxation of the fluorescent state are complex. To elucidate these mechanisms, each nucleoside/nucleotide pair has to be studied in detail. Moreover, further experimental improvements permitting us to record both reliable steady-state excitation spectra and time-resolved emission spectra over a large spectral domain have to be done. We are presently working in these directions.

Acknowledgment. Financial support from the CEA program "Toxicologie Nucléaire" and the ACI "Physicochimie de la matière complexe" is gratefully acknowledged.

References and Notes

(1) Georghiou, S.; Bradrick, T. D.; Philippetis, A.; Beechem, J. *Biophys. J.* **1996**, *70*, 1909.
(2) Rayner, D. M.; Szabo, A. G.; Loutfy, R. O.; Yip, R. W. *J. Phys. Chem* **1980**, *84*, 289.
(3) Bose, S. N.; Davies, R. J. H.; Sethi, S. K.; McCloskey, J. A. *Science* **1983**, *220*, 723.
(4) Georghiou, S.; Zhu, S.; Weidner, R.; Huang, C.-R.; Ge, G. *J. Biomol. Struct.* **1990**, *8*, 657.
(5) Nordlund, T. M.; Xu, D.; Evans, K. O. *Biochemistry* **1993**, *32*, 12090.
(6) Xu, D.-G.; Nordlund, T. M. *Biophys. J.* **2000**, *78*, 1042.
(7) Ge, G.; Georghiou, S. *Photochem. Photobiol.* **1991**, *54*, 301.
(8) Georghiou, S.; Phillips, G. R.; Ge, G. *Biopolymers* **1992**, *32*, 1417.
(9) Huang, C.-R.; Georghiou, S. *Photochem. Photobiol.* **1992**, *56*, 95.
(10) Guéron, M.; Eisinger, J.; Shulman, R. G. *J. Chem. Phys.* **1967**, *47*, 4077.
(11) Eisinger, J.; Shulman, R. G. *Science* **1968**, *161*, 1311.
(12) Vigny, P. *C. R. Acad. Sci. Paris* **1971**, *272D*, 3206.
(13) Vigny, P.; Favre, A. *Photochem. Photobiol* **1974**, *20*, 345.
(14) Vigny, P.; Duquesne, M. *Photochem. Photobiol.* **1974**, *20*, 15.
(15) Callis, P. R. *Annu. Rev. Phys. Chem* **1983**, *34*, 329.
(16) Cadet, J.; Vigny, P. The Photochemistry of Nucleic Acids. In *Bioorganic Photochemistry*; Morrison, H., Ed.; John Wiley & Sons: New York, 1990; p 1.
(17) Callis, P. R. *Chem. Phys. Lett.* **1979**, *61*, 563.
(18) Morgan, J. P.; Daniels, M. *Photochem. Photobiol.* **1980**, *31*, 207.
(19) Morgan, J. P.; Daniels, M. *J. Phys. Chem.* **1982**, *86*, 4004.
(20) Häupl, T.; Windolph, C.; Jochum, T.; Brede, O.; Hermann, R. *Chem. Phys. Lett.* **1997**, *280*, 520.
(21) Fujiwara, T.; Kamoshida, Y.; Morita, R.; Yamashita, M. *J. Photochem. Photobiol. B: Biol.* **1997**, *41*, 114.
(22) Peon, J.; Zewail, A. H. *Chem. Phys. Lett.* **2001**, *348*, 255.
(23) Gustavsson, T.; Sharonov, A.; Markovitsi, D. *Chem. Phys. Lett.* **2002**, *351*, 195.
(24) Gustavsson, T.; Sharonov, A.; Onidas, D.; Markovitsi, D. *Chem. Phys. Lett.* **2002**, *356*, 49.
(25) Pecourt, J.-M. L.; Peon, J.; Kohler, B. *J. Am. Chem. Soc.* **2001**, *123*, 10370.
(26) Verapoldi, R. A.; Mielenz, K. D. *A fluorescence standard reference material: quinine sulfate dihydrate*; U. S. Government Printing Office: Washington, DC, 1980.
(27) Nijegorodov, N.; Mabbs, R. *Spectrochim. Acta A* **2000**, *56A*, 2157.
(28) Voet, D.; Gratzer, W. B.; Cox, R. A.; Doty, P. *Biopolymers* **1963**, *1*, 193.
(29) Wilson, R. W.; Callis, P. R. *J. Phys. Chem.* **1976**, *80*, 2280.
(30) Bouvier, B.; Gustavsson, T.; Markovitsi, D.; Millié, P. *Chem. Phys.* **2002**, *275*, 75.
(31) Sobolewski, A. L.; Domcke, W.; Dedonder-Lardeux, C.; Jouvet, C. *Phys. Chem. Chem. Phys.* **2002**, *4*, 1093.
(32) Ismail, N.; Blancafort, L.; Olivucci, M.; Kohler, B.; Robb, M. A. *J. Am. Chem. Soc.* **2002**, *124*, 6818.
(33) Holmén, A.; Broo, A.; Albinsson, B.; Nordén, B. *J. Am. Chem. Soc.* **1997**, *119*, 12240.